Continued development of the ISORROPIA aerosol thermodynamic equilibrium model.

Final Project Report

1. TASKS ACCOMPLISHED

1.1 Support for ISORROPIA 1.7

ISORROPIA version 1.7 (source code + manual) has been updated, corrected and posted on the model's website (http://nenes.eas.gatech.edu/ISORROPIA). Changes to the code include:

1. Updated water activity database.
2. Bug fixes, smoother performance and code optimizations.
3. More interface routines.
4. Updated download page (with a code repository as well).

1.2 Development of the ISORROPIA-II thermodynamic model

Overview of model

The system modeled by ISORROPIA II consists of the following potential components (species in bold are new in ISORROPIA II):

Gas phase:	NH_3, HNO_3, HCl, H_2O
Liquid phase:	NH_4^+, Na^+, H^+, Cl^-, NO_3^-, SO_4^{2-}, $HNO_{3(aq)}$, $NH_{3(aq)}$, $HCl_{(aq)}$, HSO_4^-, OH^-, H_2O, **Ca^{2+}, K^+, Mg^{2+}**
Solid phase:	$(NH_4)_2SO_4$, NH_4HSO_4, $(NH_4)_3H(SO_4)_2$, NH_4NO_3, NH_4Cl, NaCl, $NaNO_3$, $NaHSO_4$, Na_2SO_4, **$CaSO_4$, $Ca(NO_3)_2$, $CaCl_2$, K_2SO_4, $KHSO_4$, KNO_3, KCl, $MgSO_4$, $Mg(NO_3)_2$, $MgCl_2$**

When the concentration of crustal species (Ca, K, Mg) is zero, routines of ISORROPIA are used, which since its original release (Nenes et al., 1998) has been substantially improved for robustness, speed and expanded to solve a wider range of problems (updates can be obtained from http://nenes.eas.gatech.edu/ISORROPIA).

The number of species and equilibrium reactions is determined by the relative abundance of each aerosol precursor (NH_3, Na, Ca, K, Mg, HNO_3, HCl, H_2SO_4) and the ambient

relative humidity and temperature. The major species potentially present are determined from the value of the following ratios:

$$R_1 = \frac{\left[NH_4^+\right]+\left[Ca^{2+}\right]+\left[K^+\right]+\left[Mg^{2+}\right]+\left[Na^+\right]}{\left[SO_4^{-2}\right]}$$

$$R_2 = \frac{\left[Ca^{2+}\right]+\left[K^+\right]+\left[Mg^{2+}\right]+\left[Na^+\right]}{\left[SO_4^{-2}\right]}$$

$$R_3 = \frac{\left[Ca^{2+}\right]+\left[K^+\right]+\left[Mg^{2+}\right]}{\left[SO_4^{-2}\right]}$$

where $\left[X\right]$ denotes the concentration of an aerosol precursor X (mol m^{-3} of air). R_1, R_2 and R_3 are termed "total sulfate ratio", "crustal species and sodium ratio" and "crustal species ratio" respectively; based on their values, 5 aerosol composition regimes are defined.

As in ISORROPIA, ISORROPIA II solves two classes of problems:

a) Forward (or "closed") problems, in which known quantities are *T*, *RH* and the total (gas + aerosol) concentrations of NH_3, H_2SO_4, Na, HCl, HNO_3, Ca, K, and Mg.

b) Reverse (or "open") problems, in which known quantities are *T*, *RH* and the precursor concentrations of NH_3, H_2SO_4, Na, HCl, HNO_3, Ca, K, and Mg in the aerosol phase.

The main improvements to the original ISORROPIA release (Nenes et al., 1998) which are included in ISORROPIA II (and in the latest release of ISORROPIA version 1.7, http://nenes.eas.gatech.edu/ISORROPIA) are:

- Gas/liquid/solid partitioning has been extended to include crustal elements which resulted in 10 more salts in the solid phase and 3 more ions in the aqueous phase.
- In addition to a thermodynamically stable state the aerosol can also be in a metastable state where no precipitate is formed (always an aqueous solution).

- The water activity database has been updated, using the output from the AIM model (http://www.hpc1.uea.ac.uk/~e770/aim.html).
- Temperature dependency of the activity coefficients is included. This has been done for both pre-calculated tables and online calculations of activity coefficients.
- The MDRH points for all the systems considered have been calculated using the GFEMN model of Ansari and Pandis (1999b).
- The activity coefficient calculation algorithm has been optimized to increase computational speed and avoid numerical errors.
- The tabulated Kusik-Meissner binary activity coefficient data have been recomputed through the online calculations for the midpoint of each ionic strength interval.
- A new subroutine has been added to provide the user with the option to "force" ISORROPIA II to conserve mass up to machine precision.

Evaluation of ISORROPIA-II

ISORROPIA II is evaluated against the predictions of SCAPE2 (Kim et al., 1993abc) for a wide range of conditions characteristic of urban, remote continental, non-urban continental and marine aerosol (Heitzenberg, 1989; Fitzgerald, 1991; Ansari and Pandis, 1999a). For urban and non-urban continental aerosol, sulfates, nitrates and ammonium are usually dominant inorganic species. Sodium and chloride often compose the majority of the marine particulate matter (usually with some crustal species and sulfates present). This classification is mainly qualitative, as mixing between aerosol types often occurs in the atmosphere.

In Fig. 1 we compare predictions of aerosol water, nitrate, chloride, ammonium, total PM and hydrogen concentrations between ISORROPIA II (stable solution, forward problem solved), and SCAPE2 for the conditions specified in Table 1. Both models predict similar amount of aerosol water content (Fig. 1a) with a normalized mean error (NME) of 13.5%. Most of this discrepancy is found in the low RH regimes (RH < 60%) where SCAPE2

predicts higher water concentration compared to ISORROPIA II. This discrepancy is attributed to a) non-convergence of SCAPE2, which is corroborated by the large CPU time required for obtaining a solution (not shown), and, b) errors in the calculations of activity coefficients (both binary and multicomponent). At low RH (i.e., low liquid water content), the aqueous solution is highly non-ideal (high ionic strengths, hence the solution highly non-linear), consequently small changes in activity coefficients may result in large changes in the dissolved species concentrations and the predictions of liquid water content. On average, at RH < 60% ISORROPIA-II predicts $I > 40$. A few cases exist (for RH > 65%) for which ISORROPIA II predicts less aerosol water than SCAPE2 (Fig. 1a); this originates from differences in aerosol nitrate which then affects water uptake. For a few marine cases, SCAPE2 predicts negligible water due to non-convergence (Fig. 1a).

In Fig. 1b, total aerosol nitrate concentrations are compared for all the input conditions of Table 1. Overall, the agreement is very good with a mean error of 16.5%. ISORROPIA II predicts non-negligible amount of nitrate for some urban cases while SCAPE2 does not. For a few non-urban continental cases ISORROPIA II underpredicts aerosol nitrate compared to SCAPE2. The sources of these discrepancies are further investigated in Fountoukis and Nenes (2007).

Aerosol chloride concentration predictions are shown in Fig. 1c where both models show similar results (NME=6.5%) with small discrepancies for a few marine cases (due to non-convergence of SCAPE2 solution) in which chloride exists in significant amount due to significant presence of sea salt particles.

For aerosol ammonium predictions (Fig. 1d), no substantial differences between the two models were found (NME = 2.1%). Discrepancies were primarily found in some non-urban continental cases which represent a sulfate-poor, ammonium-rich. Even though a few differences exist in the predicted concentrations of semi-volatile species, the total PM composition (Fig. 1e) shows very good agreement (NME=13.0%). The worst agreement between the two models was seen for H^+ predictions (Fig. 1f) with the normalized mean error significantly higher than for any other component (NME=64%). The discrepancy occurs at low RH (as it scales with water content).

Small discrepancies were found to exist between the two models under certain conditions, primarily for relative humidities between 40 and 70%. These discrepancies are mainly attributed to the solution dynamics treatment of water uptake in mutual deliquescence regions and the association of non-volatile cations with sulfate, nitrate and chloride. For all cases examined, ISORROPIA II is more than an order of magnitude faster than SCAPE2, showing robust and rapid convergence for all conditions examined, making it one of the most computationally efficient and comprehensive inorganic thermodynamic equilibrium modules available.

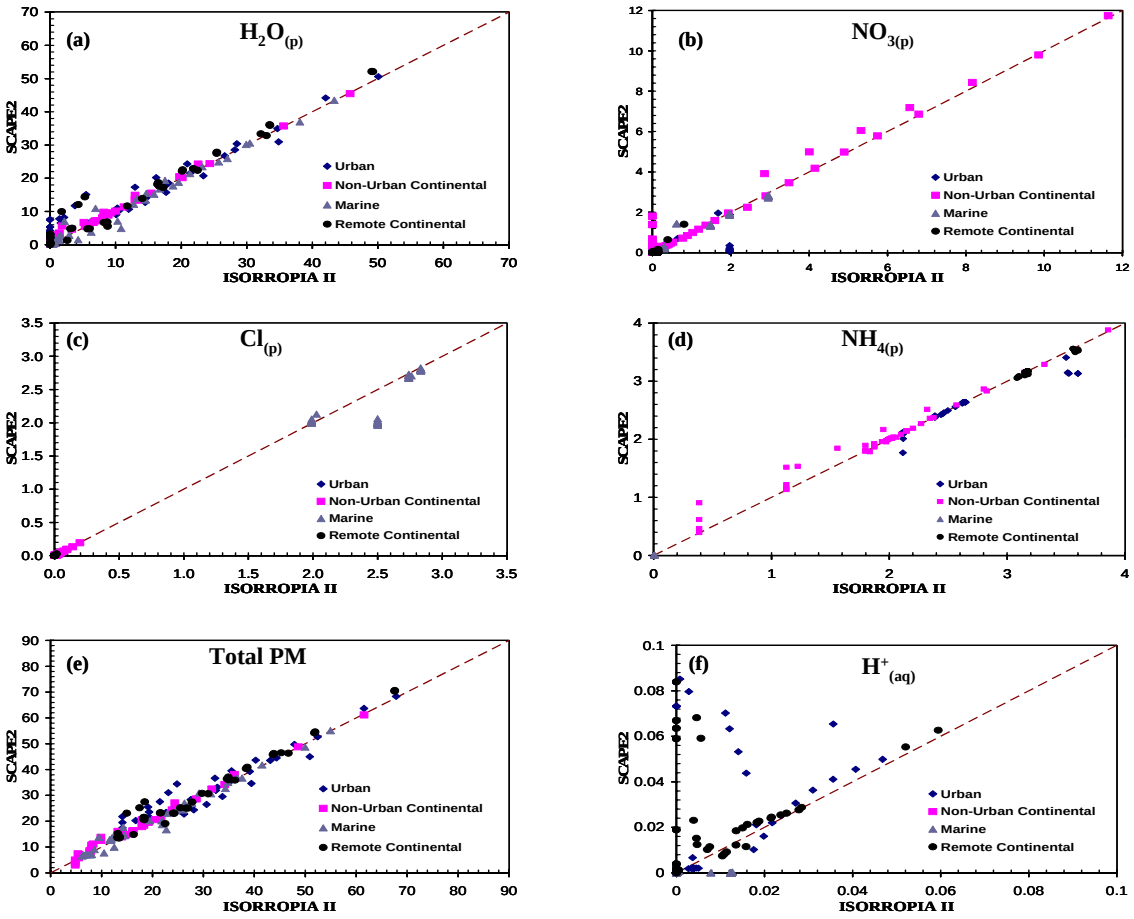

Figure 1. Concentration of aerosol water (a), nitrate (b), chloride (c), ammonium (d), total PM (e), and hydrogen (f), as predicted by ISORROPIA II (thermodynamically stable solution) and SCAPE2 for all the conditions described in Table 1. Temperature is set to 298.15K. All units are in μg m^{-3}.

Table 1. List of input conditions for model simulations[a]

Case	Aerosol Type	Na	H_2SO_4	NH_3	HNO_3	HCl	Ca^{2+}	K^+	Mg^{2+}	R_1, R_2, R_3
1	Urban (1)	0.000	10.000	3.400	2.000	0.000	0.400	0.330	0.000	2.14, 0.18, 0.18
2	Urban (2)	0.023	10.000	3.400	2.000	0.037	0.900	1.000	0.000	2.44, 0.48, 0.47
3	Urban (3)	0.000	15.000	2.000	10.000	0.000	0.900	1.000	0.000	1.27, 0.31, 0.32
4	Urban (4)	0.000	15.000	2.000	10.000	0.000	0.400	0.330	0.000	0.89, 0.12, 0.12
5	N-u Cont.[b] (1)	0.200	2.000	8.000	12.000	0.200	0.120	0.180	0.000	23.9, 0.80, 0.37
6	N-u Cont. (2)	0.100	4.000	10.000	7.000	0.100	0.120	0.180	0.050	14.8, 0.34, 0.24
7	N-u Cont. (3)	0.023	5.664	12.000	2.000	0.037	0.120	0.180	0.050	12.4, 0.18, 0.17
8	N-u Cont. (4)	0.023	5.664	20.400	0.611	0.037	0.120	0.180	0.000	20.9, 0.15, 0.13
9	Marine (1)	2.000	1.000	0.010	0.300	3.121	0.100	0.100	0.070	9.36, 9.30, 0.80
10	Marine (2)	1.500	1.000	0.010	1.500	2.500	0.360	0.450	0.050	8.66, 8.60, 2.21
11	Marine (3)	2.500	3.000	0.001	3.000	2.500	0.500	1.000	0.050	4.86, 4.86, 1.31
12	Marine (4)	3.000	3.000	0.020	2.000	3.121	0.360	0.450	0.130	5.14, 5.10, 0.84
13	Rem. Cont.[b] (1)	0.000	10.000	4.250	0.145	0.000	0.080	0.090	0.000	2.49, 0.04, 0.04
14	Rem. Cont. (2)	0.023	10.000	3.000	1.000	0.037	0.080	0.090	0.000	1.78, 0.05, 0.04
15	Rem. Cont. (3)	0.100	15.000	3.000	4.000	0.100	0.080	0.090	0.000	1.21, 0.06, 0.03
16	Rem. Cont. (4)	0.200	15.000	3.000	8.000	0.200	0.080	0.090	0.040	1.25, 0.10, 0.04

[a] Simulations for each case were conducted for 10, 25, 40, 55, 65, 70, 75, 80, 85, 90 and 98% relative humidity. Temperature was set to 298.15K. Concentration given in $\mu g\ m^{-3}$.

[b] N-u Cont., non-urban continental; Rem. Cont., remote continental.

1.3 Characterization of Mexico City Aerosol using ISORROPIA-II

In the present work, we use ISORROPIA-II, which treats the thermodynamics of the K^+-Ca^{2+}-Mg^{2+}-NH_4^+-Na^+-SO_4^{2-}-HSO_4^--NO_3^--Cl^--H_2O aerosol system, to a) concurrently test the model prediction skill and thermodynamic equilibrium assumption for the Mexico City aerosol during the MILAGRO 2006 campaign, b) gain insight on the preferred phase behavior of the aerosol (i.e. deliquescent or metastable), and, c) assess the importance of neglecting crustal species (or treating them as equivalent sodium) in thermodynamic calculations. The MILAGRO 2006 dataset analyzed here is ideal for the objectives of this study, because of significant concentrations of all the inorganic species mentioned above.

Observational data

The Megacity Initiative: Local and Global Research Observations (MILAGRO) Campaign took place in March 1 - 30, 2006 (http://www.eol.ucar.edu/projects/milagro/). The three main ground locations were: one site at the Instituto Mexicano del Petróleo (T0 site, latitude: 19.25 N, longitude: 99.10 W), another at the Universidad Tecnológica de Tecámac in the State of Mexico (T1 site, latitude: 19.703 N, longitude: 98.982 W) and a

third in Rancho La Bisnaga in the State of Hidalgo (T2 site, latitude: 20.01 N, longitude: 98.909 W). The data analyzed in this study were collected at the T1 site from 21 to 30 March 2006 and include fine particulate matter concentrations ($PM_{2.5}$) of NH_4^+, SO_4^{2-}, NO_3^-, Na^+, Cl^-, Ca^{2+}, K^+, Mg^{2+}, gas phase concentrations of NH_3, HNO_3 and ambient temperature, and relative humidity.

The $PM_{2.5}$ ion concentrations were measured by a Particle Into Liquid Sampler (PILS) with a 6-min integrated sampling period and a new chromatogram being started every 17 min. The advantage of this instrument is the simultaneous measurements of important inorganic anions and cations at high time-resolution. $NH_{3(g)}$ concentrations were obtained every minute with quantum-cascade laser (QCL) spectrometer, while volatile nitrate (i.e. $HNO_{3(g)} + NH_4NO_3$) concentrations were measured every 5 minutes by a thermal dissociation-laser induced fluorescence of nitrogen oxides (TD-LIF). Ambient temperature (T), pressure and relative humidity (RH) data are based on the measurements of the Vaisala Y50 Sensor which was operated with a 1-min time resolution. Aerosol particles ($PM_{2.5}$) were also collected (6-hour samples) with filters at the same site and sampling period.

6-minute averages of $NH_{3(g)}$ concentrations, T and RH were obtained to correspond to the 5-min averages of $HNO_{3(g)}$ and 6-min averages of $PM_{2.5}$ ion concentrations. In ~26% of the cases, the 5-min averages of $HNO_{3(g)}$ data were not coincident with the 6-min PILS concentrations, therefore a ~20-min average was considered instead (average of two measurements with a 10-min interval between the two data points). The TD-LIF measurement is the sum of gas-phase and semivolatile nitrate (i.e. $HNO_{3(g)} + NH_4NO_3$), from which $HNO_{3(g)}$ is obtained by subtracting $PM_{2.5}$ ammonium nitrate concentrations from the PILS; this can be done because preliminary ISORROPIA-II calculations suggest that the PILS nitrate is entirely semivolatile (i.e. NH_4NO_3 only). Aerosol K^+ was not accurately measured by PILS due to a calibration interference; instead, it was estimated based on a nearly constant ratio (~0.4) of K^+ to the sum of crustal species (Ca^{2+}, K^+, Mg^{2+}) obtained from the impactor data for the same site and sampling period. Gas-phase hydrochloric acid ($HCl_{(g)}$) concentrations were assumed to be zero (hence total Cl^- was equal to aerosol Cl^-). The validity of this assumption is assessed below. The measurement uncertainty was estimated to be approximately ±20%

for the PILS instrument, ±10% for the $NH_{3(g)}$ measurement, ±30% for the TD-LIF instrument and ±5% for RH. The $HNO_{3(g)}$ uncertainty, $\sigma_{HNO_{3(g)}}$, was estimated from the uncertainties of volatile $\sigma_{(TD-LIF\ nitrate)}$, and PILS nitrate $\sigma_{(PILS\ nitrate)}$, respectively, as:

$$\sigma^2_{HNO_{3(g)}} = \sigma^2_{(TD-LIF\ nitrate)} + \sigma^2_{(PILS\ nitrate)} \quad (1)$$

The reported detection limit for the PILS concentrations is 0.02 μg m^{-3} for PILS Na^+, NH_4^+, NO_3^- and SO_4^{2-}, 0.002 μg m^{-3} for PILS Ca^{2+}, Mg^{2+} and Cl^- and 0.35 μg m^{-3} for the QCL $NH_{3(g)}$ measurement.

Overall, 102 6-minute data points were obtained for which measurements of all particulate and gaseous species are available. Ammonia was predominantly in the gas phase while nitrate was dominant in the aerosol phase. The total (gas + particulate) ammonia (TA) to sulfate molar ratio was much larger than 2 (average value = 26.5) indicating sulfate poor aerosols. Relatively low concentrations of Na^+ (0.063 ± 0.113 μg m^{-3}), Ca^{2+} (0.116 ± 0.206 μg m^{-3}), K^+ (0.097 ± 0.140 μg m^{-3}) and Mg^{2+} (0.033 ± 0.051 μg m^{-3}) were detected while the total $PM_{2.5}$ mass was, on average, 28.47 ± 13.03 μg m^{-3}. Temperature did not vary significantly over the measurement period of study (mean value of 289.5 ± 5.1 K) while RH varied significantly (mean value of 58.1 ± 22.6 %), exhibiting a typical diurnal cycle which peaks in the evening and early morning and is minimum at around noon. Fig. 2 shows an example of diurnal profiles of measured ammonium, nitrate and ambient RH for March 27.

Aerosol equilibrium modeling

ISORROPIA-II is used in this study, in the forward mode of ISORROPIA-II is used. Given that there are no size-resolved data available with a temporal resolution of minutes, applying a size-resolved analysis would require numerous assumptions that would introduce rather important uncertainties. Instead, a bulk equilibrium assumption is used; although this can often lead to large prediction errors (as composition across particle sizes tend to vary), we postulate that it is a reasonable assumption for submicron Mexico City aerosol for the following reasons:

- Mexico City is unusually ammonia-rich. Most of NH_3 resides in the gas phase even after equilibration, hence particle acidity is not expected to vary substantially with size.
- Aerosol at the T1 site is often aged, hence tends to be internally mixed.
- Submicron aerosol mass in Mexico City tends to be in the 300-900 nm range, hence the equilibrium assumption can be used for those particles.

Results and discussion

Model vs. observations

In this section we evaluate the ability of ISORROPIA-II to reproduce the observed partitioning of ammonia, nitrate and chloride, which will test the expectation that equilibrium partitioning of semivolatile aerosol species is attained somewhere between 6 and 30 minutes. Fig. 3a-e shows predicted vs. observed concentrations of gas-phase ammonia ($NH_{3(g)}$), nitric acid ($HNO_{3(g)}$), aerosol phase ammonium ($NH_{4(p)}$), nitrate ($NO_{3(p)}$) and chloride ($Cl_{(p)}$), respectively; Table 2 summarizes the corresponding error metrics. For the simulations of Fig. 3, ISORROPIA-II was run in forward mode and stable state conditions. Most of the total ammonia (88.7% on average) resides in the gas phase. The data have been separated into 4 classes based on a "completeness factor" (CF). For half of the data analyzed (51%), 6-min average measurements of all (gas + particulate phase) species were available; these data are represented as "CF=0". For ~26% of the data, only 20-min average (two 6-min averages with a 10-min interval) measurement of ion concentrations from the PILS instrument were available and are "CF=1" data. Subtracting the PILS ammonium nitrate measurement from the TD-LIF (i.e. $HNO_{3(g)}$ + NH_4NO_3) occasionally resulted in a negative $HNO_{3(g)}$. Under such conditions, $HNO_{3(g)}$ is assumed zero, and the data is indicated as "CF=2" if they correspond to 6-minute averages (13% of the data), and "CF=3" for 20 min averages (10% of the data). The prediction skill of ISORROPIA is quantified in terms of five error metrics, the

normalized mean error (NME), $NME = \frac{\sum_i^n |I_i - O_i|}{\sum_i^n O_i}$, the normalized mean bias (NMB), $NMB = \frac{\sum_i^n (I_i - O_i)}{\sum_i^n O_i}$, the mean absolute gross error (MAGE), $MAGE = \frac{1}{N}\sum_i^n |I_i - O_i|$, the mean bias (MB), $MB = \frac{1}{N}\sum_i^n (I_i - O_i)$, and the root mean square error (RMSE), $RMSE = \left[\frac{1}{N}\sum_i^n (I_i - O_i)^2\right]^{1/2}$, where I_i represents predictions of ISORROPIA-II for data point i, O_i represents observations and n is the total number of data points. NME and MAGE give an estimation of the overall discrepancy (scatter) between predictions and observations, while NMB and MB are sensitive to systematic errors (biases). MAGE and MB give the error and bias respectively in μg m^{-3}, while NME and NMB in %; RMSE is the root of the mean square error, which, being the second moment of the error, incorporates both the variance of the prediction and its bias (in μg m^{-3}). Both NME and MAGE inherently include the bias which is the reason why the magnitude of NME (and MAGE) is equal or larger than NMB (and MB respectively). For an unbiased prediction, NME and MAGE express the variance. When NME and NMB (or MAGE and MB respectively) are close to each other in magnitude, the discrepancy is explained as a systematic bias rather than scatter. When the magnitude of NME/MAGE is much larger than NMB/MB, part of the discrepancy between predictions and observations is explained as scatter.

Very good agreement between model predictions and observations was found for $NH_{3(g)}$ (Fig. 3a) with a NME of 5.3%, a slope of 0.991, an intercept of -0.676 μg m^{-3} (much smaller than concentrations of $NH_{3(g)}$) and an R^2 of 0.992. When compared to the observed value (16.89 μg m^{-3}), the mean error and bias, as well as the RMSE for $NH_{3(g)}$ are notably low (0.94, -0.83 and 1.27 μg m^{-3} respectively). This is not surprising, as most of the ammonia resides in the gas phase, so $NH_{3(g)}$ is relatively insensitive to aerosol

ammonium prediction errors. Particulate ammonium (Fig. 3b) was systematically overpredicted, as shown by the 37.1% NMB and the 0.83 μg m^{-3} mean bias compared to the measured value of 2.24 μg m^{-3} (Table 2). This overprediction could arise from the phase state assumption, departure from equilibrium or measurement uncertainty; all of these possibilities are explored below.

Predictions of $HNO_{3(g)}$ were subject to significant scatter (Fig. 3c), with a NME of 80.8% and MAGE=1.46 μg m^{-3} but the bias was comparable to the other species (Table 2). The scatter is attributed to that *a*) particles larger than 2.5 μm in diameter are not included in our calculations (although too large to be in equilibrium with the gas phase, they could still react with nitric acid and introduce some prediction error), *b*) zero concentrations of $HNO_{3(g)}$ for a portion of the data (CF=2 and 3), and, *c*) low, on average, concentrations of gas phase nitrate which results in predictions of $HNO_{3(g)}$ being very sensitive to errors in particulate nitrate ($NO_{3(p)}$). When partitioning is predominantly in one phase, small errors in its predicted concentration are substantially amplified in the other phase. Additionally, the estimated uncertainty for $HNO_{3(g)}$ (using Eq. 1) was found to be roughly ~100%; the agreement between predicted and observed $HNO_{3(g)}$ is in fact within the estimated uncertainty. For particulate nitrate (Fig. 3d), ISORROPIA-II predictions agree well with observations with a NME of 27.2% and a small bias (NMB = 8.0%).

Observed concentrations of Cl^- agree well (NME=15.5%, MAGE=0.04 μg m^{-3}) with predicted values (Fig. 3e); ISORROPIA-II predicts very small amounts of chloride in the gas phase because the large excess of $NH_{3(g)}$ tends to drive Cl^- almost completely into the aerosol phase. This justifies (to first order) the assumption of effectively zero $HCl_{(g)}$ in the thermodynamic calculations. However, the NME and NMB, as well as MAGE and MB, are almost identical in magnitude; this suggests that the prediction error is likely only from the "missing" (small) amount of $HCl_{(g)}$ that are not considered in the calculations of Fig. 3e. Minimizing the NMB would require on average 0.03 μg m^{-3} gas-phase HCl (min:0, max:0.3 μg m^{-3}).

Although NMB strongly depends on the averaging time, NME does not. The same is seen for MB and MAGE respectively. This may be the residual effect of particles with

diameter larger than 2.5 μm reacting with nitrates; since coarse particles vary significantly throughout the dataset and are not included in our calculations, their effect likely manifests as "scatter" in the predictions. This suggests that up to 1.46 μg m^{-3} (MAGE value for nitrate) out of the 5.38 μg m^{-3} observed, which is roughly 30% of the unresolved particulate nitrate (also expressed as ~30% NME) could be associated with particles larger than 2.5 μm diameter.

Equilibrium timescale

Agreement between predictions and measurements depends on many factors, such as equilibrium timescale and measurement uncertainty. Fig. 3 (and Table 2) shows that the closure for CF=0 data is slightly worse than for CF=1 to 3, which could be an indication that the averaging timescale might affect the bias. Since the NMB and NME for particulate nitrate are consistent between CF classifications, this suggests that the TD-LIF provides an excellent measure of volatile nitrate. Based on work to date we expect the equilibration timescale to be ~ 20 minutes; indeed the Table 2 results support this, as NMB is consistently minimum for the 20 min data (Table 2). However, since different data correspond to different atmospheric conditions (temperature, relative humidity, time), no definite conclusion on the equilibration timescale can be drawn based on the error metrics. An equilibrium timescale and its sensitivity to changes in *RH*, *T* and aerosol precursor concentration can still be derived from the measurements. For this, we start from the mass transport equation from/to particle:

$$\frac{dm}{dt} = k(c - c_{eq}) \tag{2}$$

where k is the mass transfer coefficient, c is the ambient concentration of a species and c_{eq} is its concentration at equilibrium. k depends on the gas-phase diffusivity, D_g, and the size of the particle (Seinfeld and Pandis, 1998),

$$k = \frac{3D_g}{R_p^2} \tag{3}$$

where R_p is the effective radius of the particle. k also depends on the mass accommodation coefficient, α, but for values of $\alpha > 0.1$ the mass transfer rate is not

sensitive to the exact value of α (Seinfeld and Pandis, 1998). D_g was calculated from the Chapman-Enskog theory for binary diffusivity and was found to be 0.2 cm^2s^{-1} for NH_3 and 0.14 cm^2s^{-1} for HNO_3 (average for the conditions of T and P observed during the measurement period).

Assuming that c changes with time, with a rate obtained from observations, $c = c_o + \left(\frac{dc}{dt}\right)t$, where c_o is the observed concentration at time t_o. Substituting into Equation (2) gives:

$$\frac{dm}{dt} = k\left\{c_o + \left(\frac{dc}{dt}\right)t - c_{eq}\right\} = k\left\{c_o - c_{eq}\right\} + k\left(\frac{dc}{dt}\right)t \tag{4}$$

The characteristic time for equilibrium establishment can be estimated by scaling Eq. (4). If the characteristic aerosol mass concentration is m_p and the characteristic timescale is τ_{eq} one can scale t, m as $t' = \frac{t}{\tau_{eq}}$ and $m' = \frac{m}{m_p}$, respectively. Substitution into Eq. 4 gives,

$$\frac{m_p}{\tau_{eq}}\frac{dm'}{dt'} = k\left\{c_o - c_{eq}\right\} + k\left(\frac{dc}{dt}\right)t'\tau_{eq} \tag{5}$$

Assuming that $\frac{m_p}{\tau_{eq}} \approx k\left(\frac{dc}{dt}\right)\tau_{eq}$ a characteristic equilibrium timescale can be defined as,

$$\tau_{eq} = \left(\frac{m_p}{k\,\Delta c/\Delta t}\right)^{1/2} \tag{6}$$

where Δc, Δt are the changes in concentration and time, respectively, between two consecutive measurements.

Assuming a particle density of 1.0 g cm^{-3} (characteristic for deliquesced aerosol exposed to high RH) a mass accommodation coefficient of 0.1 for gas-phase NH_3, HNO_3 and an aerosol diameter of 1 μm, the timescale for equilibrium for all semivolatile species is computed using Eq. 6. As can be seen in Fig.4, semivolatile partitioning equilibrates (on average) on a timescale between 15 – 30 min (Fig 4a,b) during the measurement period of March 21 - 30 (27±19 min for HNO_3, 14±11 min for NH_3, 18±15 min for NO_3 and 15±13 min for NH_4, on average). The equilibration timescale for NH_3 is close to that of

NH_4, and, the timescale of HNO_3 is close to that of NO_3, despite that they include independent measurements of aerosol and gas-phase precursors; this strongly suggests consistency in the timescale analysis. Interestingly, by focusing on specific days, one can notice a systematic diurnal cycle of the equilibration timescale. Figure 4c shows the timescale of NH_4 and NO_3 for two days (March 28 and 29). The timescale reaches a maximum during midnight, when T is lower, RH is high and concentrations of species are high (because of the collapse of the boundary layer). Increasing the particle diameter to 2 μm increases the timescales by a factor of 2, while an increase in aerosol density from 1 to 2 g cm^{-3} increases the equilibration timescale by ~40% (not shown).

It is also important to evaluate the influence of environmental changes to the equilibration timescale. This is done by evaluating the instantaneous τ_{eq} (computed from c_o, RH_o, T_o) against changes from fluctuations in c, RH and T. The effect of $\left(\frac{dc}{dt}\right)$ is already expressed in Equation 5; the effects of RH and T through their effects in equilibrium composition,

$$c_{eq} = c_{eq,o} + \frac{\partial C_{eq}}{\partial RH} dRH + \frac{\partial C_{eq}}{\partial T} dT \tag{7}$$

Introduction of Equation 7 into 4 gives:

$$\begin{aligned} \frac{dm}{dt} &= k\left\{ c_o - \left(c_{eq,o} + \frac{\partial C_{eq}}{\partial RH} dRH + \frac{\partial C_{eq}}{\partial T} dT \right) \right\} + k\left(\frac{dc}{dt}\right)t \\ &= k\left(c_o - c_{eq,o}\right) - k\left(\frac{\partial C_{eq}}{\partial RH} dRH\right) - k\left(\frac{\partial C_{eq}}{\partial T} dT\right) + k\left(\frac{dc}{dt}\right)t \end{aligned} \tag{8}$$

The terms on the right hand side of Equation (8) express (from left to right) the rate of change of particle mass from the instantaneous departure of concentration from equilibrium, the effect of *RH* change, *T* change, and, aerosol precursor change. The latter 3 are affected by changes in environmental conditions, and the first term expresses the instantaneous equilibration timescale. Because of this, one can define the ratios of timescales as:

$$\frac{\tau_{eq}}{\tau_{RH}} = \left(\frac{\frac{\partial C_{eq}}{\partial RH} dRH}{\left(c_o - c_{eq,o}\right)} \right) \approx \left(\frac{\frac{\partial C_{eq}}{\partial RH} \Delta RH}{\left(c_o - c_{eq,o}\right)} \right) \quad (9)$$

Where $\frac{\partial C_{eq}}{\partial RH}$ is the sensitivity of equilibrium concentration to changes in *RH* (calculated from ISORROPIA-II, by evaluating the equilibrium solution at RH_o, and, RH_o+0.01) and ΔRH is the observed change in *RH* between two consecutive measurements. Similarly, one can define the ratio of timescales of instantaneous equilibration to *T* variations as:

$$\frac{\tau_{eq}}{\tau_T} = \left(\frac{\frac{\partial C_{eq}}{\partial T} dT}{\left(c_o - c_{eq,o}\right)} \right) \approx \left(\frac{\frac{\partial C_{eq}}{\partial T} \Delta T}{\left(c_o - c_{eq,o}\right)} \right) \quad (10)$$

Where $\frac{\partial C_{eq}}{\partial T}$ is the sensitivity of equilibrium concentration to changes in *T* (calculated from ISORROPIA-II, by evaluating the equilibrium solution at T_o, and, T_o+0.1), and, ΔT is the observed change in *T* between two consecutive measurements.

Finally, one can define the ratio of instantaneous equilibration timescale to the rate of change of precursor as:

$$\frac{\tau_{eq}}{\tau_C} = \left(\frac{\left(\frac{dc}{dt}\right) dt}{\left(c_o - c_{eq,o}\right)} \right) \approx \left(\frac{\Delta c}{\left(c_o - c_{eq,o}\right)} \right) \quad (11)$$

where Δc is the change in precursor concentration between two consecutive measurements.

If $\left\{ \frac{\tau_{eq}}{\tau_C}, \frac{\tau_{eq}}{\tau_T}, \frac{\tau_{eq}}{\tau_{RH}} \right\} < 1$, then the equilibrium timescale is dominated by transients in ambient concentration, *RH*, *T* and vice versa. Fig. 4 shows the calculated timescale ratios for gas-phase HNO_3, NH_3 and aerosol NO_3, NH_4 during the measurement period of March 21-30, 2006. If *c*, *RH* and *T* change slowly enough, the timescale ratios are much larger than 1; this was found to frequently apply in the dataset (88% for NH_3, 58% for NH_4, 55% for HNO_3 and 75% for NO_3). This suggests that calculation of the equilibrium

timescale based on instantaneous values of c, RH, T is representative. For times where the ratio was less than unity, $\frac{\tau_{eq}}{\tau_C}$ was almost always larger than $\frac{\tau_{eq}}{\tau_T}$ and $\frac{\tau_{eq}}{\tau_{RH}}$. This suggests that τ_c is less than τ_{RH} or τ_T, meaning that changes in RH and T affect the equilibration timescale more strongly than changes in aerosol precursor concentration.

Deliquescence vs. Metastable state

Due to the hysteresis effect, there is always an issue on what is the appropriate thermodynamic state assumption for RH < 60%, where crystallization may occur. This dataset covers a wide range of RH (19-94%) and makes it possible to assess the preferred phase transition path (i.e. deliquescence or metastable branch) for Mexico City aerosol. In Fig. 6 we plot the stable ("deliquescence") and metastable ("metastable") solution predictions of ISORROPIA-II compared to observations for $NH_{4(p)}$ and $NO_{3(p)}$ as a function of RH for the whole dataset (March 21-30). The stable state solution of ISORROPIA-II predicts higher concentrations of aerosol ammonium and aerosol nitrate at RH <50%. At low RH (<50%), the stable state solution predicts a solid phase consisting mainly of $(NH_4)_2SO_4$ and NH_4NO_3. The metastable state solution assumes the particulates are composed of an aqueous supersaturated solution throughout the whole RH regime; hence no solid NH_4NO_3 is allowed to form. At RH >50%, solid NH_4NO_3 dissolves and "stable" and "metastable" aerosol predictions become identical. This can also be seen in Fig. 7, which presents the observed and predicted (by both solutions of ISORROPIA-II) aerosol nitrate diurnal profile for March. During the early morning and night, when RH is high, both solutions predict the same concentration. For periods of high RH, the model slightly overpredicts the measured particulate nitrate concentrations, while at low RH (<30%) it generally underpredicts. Possible reasons for this could be the presence of WSOC influencing the partitioning of inorganic species between the gas and aerosol phase (not considered by ISORROPIA-II) or the high measurement uncertainty in RH at high values. The existence of other species (not modeled) by ISORROPIA-II would lower the mutual deliquescence point and increase the amount of dissolved nitrate in the aerosol phase at low RH.

The differences between stable and metastable solutions predictions shown in Fig. 3 are quantified in Table 3; NME, NMB, MAGE and MB are computed only for data with RH < 50%. For aerosol ammonium, although the NME (and MAGE) for the two solutions of ISORROPIA II is essentially the same, the opposite sign in NMB and MB (Table 3), indicates an overprediction (+11%) of ammonium by the stable state and an underprediction (-9%) by the metastable solution. The systematic overprediction of ammonium by the stable solution (seen in Fig. 3) may partially reflect measurement uncertainty. For aerosol nitrate, the error and bias between predictions and observations is significantly larger when using the metastable solution (NME=47.4%, NMB=-46.4%, MAGE=2.8μg m^{-3}, MB=-2.74μg m^{-3}) of ISORROPIA II compared to the stable state solution (NME=25.8%, NMB=-18.5%, MAGE=1.5μg m^{-3}, MB=-1.1μg m^{-3}) for RH < 50%, suggesting that aerosols in Mexico City prefer the deliquescence branch of the phase diagram. However, Moya et al. (2007) showed that the metastable branch gives better agreement between predictions and observations at low RH during the MER 2005 campaign (Mexico City downtown). An important difference between the two datasets is the sulfate-to-nitrate (SO_4^{2-}/NO_3^-) molar ratio, being larger than unity for the MER data and less than unity for the current dataset (on average $SO_4^{2-}/NO_3^- \approx 0.7$). Since a subset of the current dataset exhibited a SO_4^{2-}/NO_3^- larger than 1, we examine the possibility that particulate SO_4^{2-}/NO_3^- correlates with a change in the preferred phase state for RH below 50%. In Table 4 we show the performance of both stable and metastable solution of ISORROPIA-II at RH below 50% and for aerosol SO_4^{2-}/NO_3^- ratio larger and less than 1. At aerosol $SO_4^{2-}/NO_3^- < 1$, NME and NMB are much larger in the metastable solution for $HNO_{3(g)}$ and $NO_{3(p)}$ and slightly larger for $NH_{3(g)}$ and $NH_{4(p)}$ while for aerosol $SO_4^{2-}/NO_3^- > 1$ the opposite is seen (although with much smaller differences in NMB between the two solutions). The results of this study, combined with Moya et al. (2007) suggest that the stable state is preferred when $SO_4^{2-}/NO_3^- < 1$ and vice versa. However, this serves only as an indication, as there is relatively few data (12 points) for which $SO_4^{2-}/NO_3^- > 1$ at RH < 50%. More data are needed to further substantiate this hypothesis.

The existence of metastable aerosol for low RH may seem at first surprising, particularly since crustal species, which tend to promote efflorescence under supersaturated conditions, are present. If substantial amounts of predicted solid $CaSO_4$ is

used as a proxy for crustal influence, only 25% of the points for which $SO_4/NO_3 > 1$ are influenced; 48% of the data are influenced when $SO_4/NO_3<1$. This suggests that crustals may indeed influence the phase state of aerosol, although organic compounds (not considered by ISORROPIA-II) can form eutectic mixtures that contain thermodynamically stable water down to very low relative RH, thus giving the "appearance" of a metastable state. Unfortunately, there were no in-situ measurements of particle phase state or size-resolved compositional data available with the time resolution required to further support our results, although the model suggests the semi-volatile inorganic partitioning is mostly consistent with a metastable state whenever dust is not present in significant amounts.

Sensitivity of Model Predictions to Aerosol Precursor Concentrations

In this section we explore the sensitivity of predictions to aerosol precursor concentrations to a) assess the importance of measurement uncertainty on predictions, and, b) assess the sensitivity of $PM_{2.5}$ to changes in emitted precursors. The sensitivity is assessed by perturbing the input concentrations of total ammonia (TA), total nitrate (TN), total sulfate (TS), crustals and sodium by ±20% (approximately the PILS measurement uncertainty). The results of this analysis are shown in Table 5. A 20% increase in TS does not improve the agreement between predictions and observations; in fact, a slight increase of the NME was found for ammonia and nitrate. Since the impactor data showed ~40% (on average) higher TS than the PILS (not shown), we further perturb TS by 40%, but NME does not decrease (67.9% for $NH_{4(p)}$ and 27.8% for $NO_{3(p)}$). A +20% perturbation in crustals and sodium concentrations however, slightly improved predictions of $NH_{3(g)}$ and $NH_{4(p)}$ and decreased the observed overprediction seen in Fig. 3b; this is because crustals and sodium preferentially neutralize sulfates, so less ammonia binds to form $(NH_4)_2SO_4$ which decreases the predicted $NH_{4(p)}$ concentration and increases the amount of $NH_{3(g)}$. In fact, the impactor data suggest that Ca^{2+}, Mg^{2+} and Na^{2+} are much higher (approximately 4 times) than obtained with the PILS. Increasing crustals and sodium by a factor of 4 significantly decreases the systematic error between predictions and measurements for particulate ammonium (NMB = 13.6%); predictions

for $NH_{3(g)}$ (mean predicted value = 17.42 μg m^{-3}) and $NH_{4(p)}$ (mean predicted value = 2.55 μg m^{-3}) are improved. This implies that the PILS in this dataset may not account for all the crustals present in $PM_{2.5}$.

In Fig. 8 we plot the predicted change (%) in $PM_{2.5}$ nitrate as a function of RH when a 20% decrease in input concentrations of TA, TS and TN is applied. The nitrate response to sulfate is negligible, Δx=0.36%, (Fig. 8, Table 5) because TA concentrations are substantially in excess, and, thus a 20% change in TS is not enough to affect the formation of ammonium nitrate. (In an ammonia-limited environment, a reduction in sulfate would increase aerosol nitrate as ammonia is freed and allowed to react with nitric acid). As seen in Fig. 8, nitrate predictions are sensitive to changes in TA only for RH < 60%. This is expected since below the deliquescence point of NH_4NO_3 the partitioning of nitrate is strongly dependent on the ammonia vapor pressure and thus reducing TA reduces the amount of NH_4NO_3 formed. At RH > 60%, nitrate is mostly dissolved and unaffected by the changes in TA. Aerosol nitrate predictions are more directly influenced by reductions in TN as shown in Fig. 8 and Table 5 (Δx=-22.8%), and is in agreement with Takahama et al., (2004). The sensitivity of aerosol nitrate is RH-dependent as the partitioning of nitrate strongly depends on the amount of aerosol water.

Importance of Explicitly Treating Crustal Species

Often thermodynamic models treat the presence of crustals as mole-equivalent sodium (i.e. $Ca^{2+} = 2Na^{+}$, $Mg^{2+} = 2Na^{+}$, $K^{+} = Na^{+}$) or as insoluble. In this section we examine the impact of these assumptions, versus using full thermodynamics. Table 6 displays a summary of this sensitivity test; shown are average concentrations and error metrics for nitrate, ammonium and water with ISORROPIA-II. For all the simulations we used the concentrations of crustals and sodium from the impactor data. When Ca^{2+}, K^{2+} and Mg^{2+} are treated as insoluble (unreactive), ISORROPIA-II predicts higher, on average, concentrations of ammonium compared to both the equivalent-Na and explicit treatment, since more sulfate is available to bind with ammonium, and thus the error and bias between predicted and observed ammonium increases for the insoluble approach (Table 6). For particulate nitrate, NME, NMB, MAGE and MB are the lowest when

crustals are treated explicitly. The changes in NME and NMB among the three crustal treatment approaches are rather small since ammonia is enough to fully neutralize the available nitrate regardless of the treatment of crustals. The difference in nitrate prediction when treating crustals explicitly vs. as equivalent sodium is expected to be large in environments where non-volatile nitrate ($Ca(NO_3)_2$, $Mg(NO_3)_2$, KNO_3) is present in significant amounts. In the current dataset, aerosol nitrate is present in the form of ammonium nitrate (due to ammonia-rich environment) and thus replacing crustals with sodium is expected to have a minor effect on predicted nitrate response, primarily from differences in predicted water uptake (Table 6). The equivalent Na approach predicts aerosol water content which is higher (by 13.5%) than the one predicted by the explicit treatment of crustals and very close to the insoluble approach (Table 6). This is attributed to the formation of salts with low solubility (e.g., $CaSO_4$) which does not significantly contribute to water uptake. The difference in water content also affects aerosol acidity (i.e. pH) and water-soluble species concentration. It should be noted that the differences described in Table 6 between the equivalent Na and explicit treatment of crustals are the minimum expected considering the large amounts of ammonia in Mexico City which minimizes the effect of replacing crustals with sodium.

Conclusions

In agreement with observations, ISORROPIA-II predicts that ammonia (82.4 ± 10.1 %) primarily resides in the gas phase, while most of total nitrate (79.8 ± 25.5%) and chloride (75.3 ± 29.1%) resides in the aerosol phase. The mean observed value for $NH_{3(g)}$ was 17.73 μg m^{-3} and 5.37 μg m^{-3} for $NO_{3(p)}$. An excellent agreement between predicted and observed concentration of $NH_{3(g)}$ was found with a NME of 5.3%. Very good agreement was also found for $NO_{3(p)}$ (NME=27.2%), $NH_{4(p)}$ (NME=37.1%) and $Cl_{(p)}$ (NME=15.5%) concentrations for most of the data. Larger discrepancies were seen in predicted $HNO_{3(g)}$ since uncertainties in the volatile nitrate measurement ($HNO_{3(g)}$ + NH_4NO_3) are magnified by the high sensitivity of $HNO_{3(g)}$ because nitrate partitioned primarily to the aerosol phase. A number of important conclusions arise from this study:

1. Application of ISORROPIA-II is largely successful, suggesting that the assumption of bulk thermodynamic equilibrium is to first order applicable (i.e. to with 20% of measured concentrations) for Mexico City fine aerosol particulate matter. We suggest that this happens because *i*) Mexico City is unusually ammonia-rich, so most of it resides in the gas phase even after equilibration – hence particle acidity is not expected to vary substantially with size (aerosol nitrate is not systematically underpredicted, which further supports that acidity does not vary substantially between submicron particles), *ii*) aerosol at T1 is generally aged and its aerosol heterogeneity is expected to be much less, when compared to aerosol collected from downtown (T0).

2. Assuming a particle diameter of 1 μm, the timescale for thermodynamic equilibrium of semi-volatile species was found to be 27±19 min for HNO_3, 14±11 min for NH_3, 18±15 min for NO_3 and 15±13 min for NH_4, on average with a maximum during the night and early morning hours. Changes in RH and temperature tend to affect the equilibration timescale more than changes in aerosol precursor concentration.

3. The scatter in nitrate prediction error (~30%) can be attributed to reaction of particles between 2.5 and 10 μm diameter with nitrate (the effect of which is not considered in our analysis). If true, this suggests that on average, up to 30% of the total aerosol nitrate can be associated with particles having diameter larger than 2.5 μm.

4. At low RH (<50%), the stable state (i.e. deliquescence branch) solution of ISORROPIA-II predicted significantly higher concentrations of aerosol nitrate compared to the metastable solution. Further analysis indicates this to be true when $SO_4^{2-}/NO_3^- < 1$. The opposite was seen (although with a much smaller difference between metastable and stable predictions) when $SO_4^{2-}/NO_3^- > 1$. This bimodal behavior may be a result of crustal influence, which may at times be diminished by organics that can promote thermodynamically stable water down to very low relative RH. This can serve as an important constraint for three dimensional air quality models that simulate ambient particle concentrations under conditions characteristic of Mexico City.

5. The volatile fraction of $PM_{2.5}$ was found to be mostly sensitive to changes in TN. This suggests that in an ammonia-rich environment, (such as Mexico City) a combined reduction in TS and TN (rather than TA) appears to be most effective in reducing $PM_{2.5}$ (on a mol per mol basis).

6. Treating crustal species as "equivalent sodium" (or insoluble) has an important impact on predicted aerosol water uptake, nitrate and ammonium, despite the ammonia-rich environment of Mexico City. This suggests that explicit treatment of crustals (when present) is required for accurate predictions of aerosol partitioning and phase state.

7. Concentrations of gas phase HCl were most likely low (mean predicted value for $HCl_{(g)}$=0.03 μg m^{-3}), a consequence of having large excess of $NH_{3(g)}$ which tends to drive Cl^- into the aerosol.

Table 2. Comparison between predicted and observed concentrations of semivolatile species during the MILAGRO 2006 (21-30 March) campaign. Simulations are done assuming the aerosol can form solids ("stable" solution).

Data Type	Quantity	$NH_{3(g)}$	$NH_{4(p)}$	$HNO_{3(g)}$	$NO_{3(p)}$	$HCl_{(g)}$	$Cl_{(p)}$
All data (102 data)	mean observed (μg m^{-3})	17.73 ± 11.02	2.24 ± 1.22	1.81 ± 1.88	5.37 ± 3.57	-	0.25 ± 0.56
	mean predicted (μg m^{-3})	16.89 ± 10.97	3.08 ± 1.56	1.38 ± 1.92	5.8 ± 3.86	0.03 ± 0.11	0.22 ± 0.55
	NME (%)	5.3	42.0	80.9	27.2	-	15.6
	NMB (%)	-4.7	37.1	-23.8	8.0	-	-15.6
	MAGE (μg m^{-3})	0.94	0.94	1.46	1.46	-	0.04
	MB (μg m^{-3})	-0.83	0.83	-0.43	0.43	-	0.04
	RMSE (μg m^{-3})	1.27	1.27	2.02	2.02	-	0.12
CF=0 (51 data)	mean observed (μg m^{-3})	17.33 ± 9.83	2.37 ± 1.18	2.63 ± 1.87	5.57 ± 3.50	-	0.28 ± 0.56
	mean predicted (μg m^{-3})	16.16 ± 9.88	3.54 ± 1.57	1.43 ± 1.98	6.76 ± 3.77	0.04 ± 0.12	0.25 ± 0.55
	NME (%)	7.2	52.3	71.7	33.9	-	17.6
	NMB (%)	-6.7	49.2	-45.5	21.5	-	-17.6
	MAGE (μg m^{-3})	1.24	1.24	1.89	1.89	-	0.05
	MB (μg m^{-3})	-1.17	1.17	-1.20	1.20	-	-0.05
	RMSE (μg m^{-3})	1.61	1.61	2.49	2.49	0.13	0.08
CF=1 (26 data)	mean observed (μg m^{-3})	17.05 ± 12.38	1.83 ± 0.84	1.86 ± 1.64	3.88 ± 1.99	-	0.10 ± 0.30
	mean predicted (μg m^{-3})	16.49 ± 12.23	2.39 ± 1.07	1.73 ± 2.32	4.00 ± 2.36	0.01 ± 0.05	0.09 ± 0.29
	NME (%)	4.4	41.1	63.1	30.3	-	13.0
	NMB (%)	-3.3	30.4	-6.8	3.3	-	-13.0
	MAGE (μg m^{-3})	0.75	0.75	1.17	1.17	-	0.01
	MB (μg m^{-3})	-0.56	0.56	-0.13	0.13	-	-0.01
	RMSE (μg m^{-3})	0.91	0.91	1.38	1.38	0.05	0.03
CF=2 (14 data)	mean observed (μg m^{-3})	16.63 ± 8.27	2.54 ± 1.71	0.00	7.31 ± 4.89	-	0.28 ± 0.33
	mean predicted (μg m^{-3})	16.25 ± 8.09	2.92 ± 1.83	0.98 ± 1.14	6.32 ± 5.30	0.06 ± 0.17	0.24 ± 0.30
	NME (%)	3.0	19.4	-	13.5	-	23.9
	NMB (%)	-2.3	15.0	-	-13.5	-	-23.9
	MAGE (μg m^{-3})	0.49	0.49	0.98	0.98	-	0.07
	MB (μg m^{-3})	-0.38	0.38	0.98	-0.98	-	-0.07
	RMSE (μg m^{-3})	0.68	0.68	1.47	1.47	0.18	0.09
CF=3 (11 data)	mean observed (μg m^{-3})	22.47 ± 15.43	2.27 ± 1.41	0.00	5.70 ± 4.05	-	0.48 ± 1.06
	mean predicted (μg m^{-3})	21.99 ± 15.16	2.74 ± 1.64	0.73 ± 1.05	4.96 ± 4.03	0.02 ± 0.06	0.46 ± 1.05
	NME (%)	2.3	23.2	-	12.9	-	5.8
	NMB (%)	-2.1	21.0	-	-12.9	-	-5.8
	MAGE (μg m^{-3})	0.53	0.53	0.73	0.73	-	0.03
	MB (μg m^{-3})	-0.48	0.48	0.73	-0.73	-	-0.03
	RMSE (μg m^{-3})	0.64	0.64	1.24	1.24	-	0.01

Table 3. Prediction skill metrics of ISORROPIA-II, for stable and metastable solutions. Data is shown for RH < 50%.

Aerosol state	Metric	$NH_{3(g)}$	$NH_{4(p)}$	$HNO_{3(g)}$	$NO_{3(p)}$
Stable (37 data)	NME (%)	3.6	24.3	67.7	25.8
	NMB (%)	-1.6	11.0	48.5	-18.5
	MAGE (μg m^{-3})	0.5	0.5	1.5	1.5
	MB (μg m^{-3})	-0.2	0.2	1.1	-1.1
Metastable (37 data)	NME (%)	3.6	24.3	124.3	47.4
	NMB (%)	1.3	-9.0	121.6	-46.4
	MAGE (μg m^{-3})	0.50	0.50	2.80	2.80
	MB (μg m^{-3})	0.20	-0.20	2.74	-2.74

Table 4. Prediction skill metrics of ISORROPIA-II, for stable and metastable solutions. Data is shown for RH < 50% and for sulfate-to-nitrate molar ratio larger and less than unity.

Solution Type	Error Metric	$NH_{3(g)}$	$NH_{4(p)}$	$HNO_{3(g)}$	$NO_{3(p)}$
		$SO_4/NO_3>1$			
Stable (12 data)	NME (%)	4.9	38.7	28.8	41.5
	NMB (%)	0.6	-4.7	24.9	-35.8
	MAGE (μg m^{-3})	0.76	0.76	0.89	0.89
	MB (μg m^{-3})	0.09	-0.09	0.76	-0.76
Metastable (12 data)	NME (%)	4.4	35.2	27.0	38.8
	NMB (%)	0.5	-3.9	23.0	-33.1
	MAGE (μg m^{-3})	0.69	0.69	0.83	0.83
	MB (μg m^{-3})	0.08	-0.08	0.71	-0.71
		$SO_4/NO_3<1$			
Stable (25 data)	NME (%)	3.0	21.2	82.1	24.3
	NMB (%)	-2.1	14.7	56.2	-16.6
	MAGE (μg m^{-3})	0.49	0.49	1.59	1.59
	MB (μg m^{-3})	-0.34	0.34	1.09	-1.09
Metastable (25 data)	NME (%)	3.1	21.8	159.0	47.0
	NMB (%)	1.1	-7.7	155.4	-46.0
	MAGE (μg m^{-3})	0.50	0.50	3.09	3.09
	MB (μg m^{-3})	0.18	-0.18	3.02	-3.02

Table 5. Sensitivity of volatile species to aerosol precursor concentrations

	Statistics	$NH_{3(g)}$	$NH_{4(p)}$	$HNO_{3(g)}$	$NO_{3(p)}$	$HCl_{(g)}$	$Cl_{(p)}$
base case	mean observed ($\mu g\ m^{-3}$)	17.73	2.24	1.81	5.37	-	0.25
	mean predicted ($\mu g\ m^{-3}$)	16.89	3.08	1.38	5.80	0.03	0.22
	NME (%)	5.3	42.0	80.9	27.2	-	15.6
	NMB (%)	-4.7	37.1	-23.8	8.0	-	-15.6
(+20%) TS	mean predicted ($\mu g\ m^{-3}$)	16.57	3.40	1.40	5.78	0.03	0.22
	NME (%)	6.9	54.6	81.9	27.5	-	15.5
	NMB (%)	-6.5	51.5	-22.5	7.6	-	-15.5
	Δx^* (%)	-1.91	10.50	1.68	-0.40	-	0.12
(-20%) TS	mean predicted ($\mu g\ m^{-3}$)	17.21	2.76	1.36	5.82	0.04	0.21
	NME (%)	4.0	31.5	79.9	26.9	-	15.7
	NMB (%)	-2.9	23.0	-25.0	8.4	-	-15.7
	Δx^* (%)	1.88	-10.34	-1.50	0.36	-	-0.15
(+20%) TN	mean predicted ($\mu g\ m^{-3}$)	16.53	3.44	1.46	7.15	0.03	0.22
	NME (%)	7.1	56.2	83.9	41.1	-	15.3
	NMB (%)	-6.8	53.4	-19.0	33.1	-	-15.3
	Δx^* (%)	-2.16	11.83	6.33	23.24	-	0.29
(-20%) TN	mean predicted ($\mu g\ m^{-3}$)	17.25	2.72	1.26	4.48	0.04	0.21
	NME (%)	4.1	32.3	77.0	30.5	-	15.9
	NMB (%)	-2.7	21.2	-30.1	-16.6	-	-15.9
	Δx^* (%)	2.11	-11.61	-8.22	-22.80	-	-0.40
(+20%) TA	mean predicted ($\mu g\ m^{-3}$)	20.82	3.14	1.15	6.03	0.03	0.22
	NME (%)	17.6	43.3	75.4	25.4	-	14.8
	NMB (%)	17.5	39.9	-36.5	12.3	-	-14.8
	Δx^* (%)	23.27	2.04	-16.63	3.95	-	0.96
(-20%) TA	mean predicted ($\mu g\ m^{-3}$)	12.98	2.99	1.69	5.49	0.04	0.21
	NME (%)	26.7	40.3	88.9	29.9	-	16.8
	NMB (%)	-26.7	33.3	-6.4	2.2	-	-16.8
	Δx^* (%)	-23.13	-2.80	22.83	-5.42	-	-1.45
(+20%) Na^+, Ca^{2+}, K^+, Mg^{2+}	mean predicted ($\mu g\ m^{-3}$)	16.94	3.02	1.39	5.77	0.04	0.21
	NME (%)	5.1	40.3	80.4	27.1	-	16.0
	NMB (%)	-4.4	35.0	-22.5	7.6	-	-16.0
	Δx^* (%)	0.29	-1.57	1.68	-0.40	-	-0.47

* Δx denotes the % change of the mean predicted value of each species compared to the base case prediction.

Table 6. Effect of crustal treatment on predicted concentrations of ammonium, nitrate and water.

Property	Treatment of crustals	$NH_{4(p)}$	$NO_{3(p)}$	$H_2O_{(liq)}$
mean observed (μg m^{-3})		2.24	5.37	-
mean predicted (μg m^{-3})	Insoluble	3.17	5.47	13.23
	Equivalent Na	2.77	5.61	13.09
	ISORROPIA-II	2.55	5.86	11.67
NME (NMB), (%)	Insoluble	46.8 (41.5)	31.0 (1.9)	N/A
	Equivalent Na	34.3 (23.3)	28.7 (4.4)	N/A
	ISORROPIA-II	34.0 (13.6)	26.2 (0.2)	N/A
MAGE (MB), μg m^{-3}	Insoluble	1.05 (0.93)	1.67 (0.10)	N/A
	Equivalent Na	0.77 (0.52)	1.54 (0.24)	N/A
	ISORROPIA-II	0.76 (0.31)	1.41 (0.05)	N/A

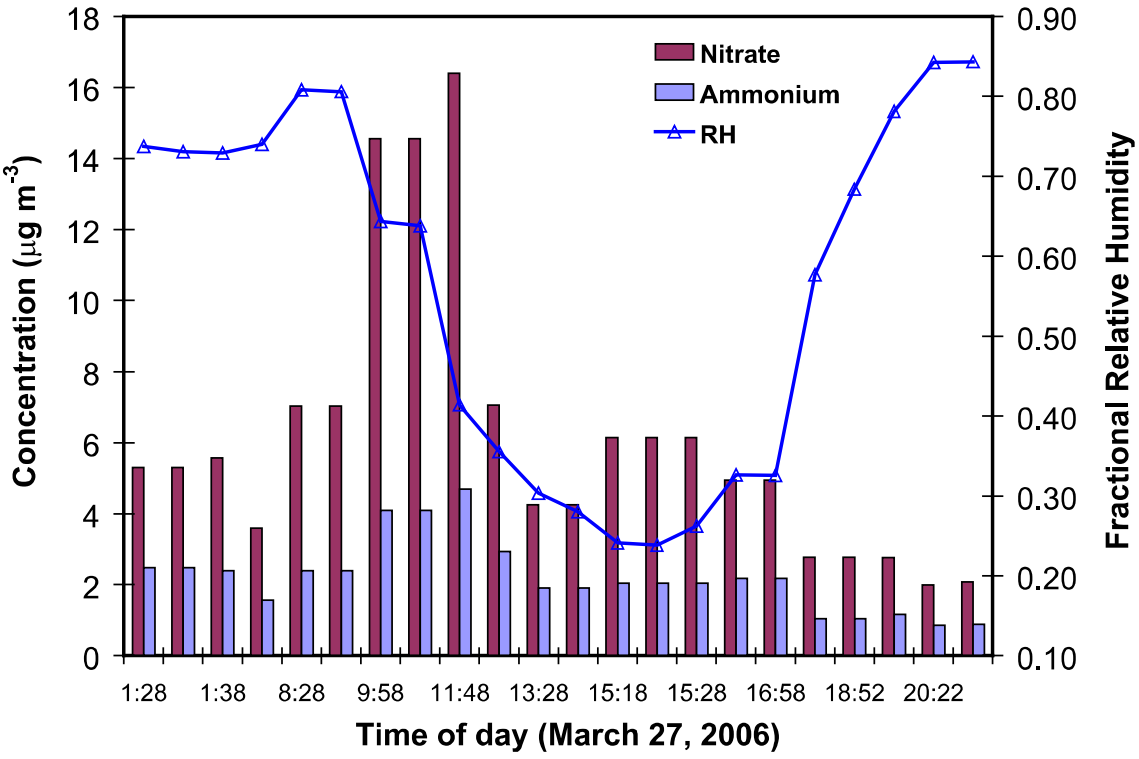

Figure 2. Diurnal profile of measured nitrate, ammonium and ambient RH for 27 March 2006.

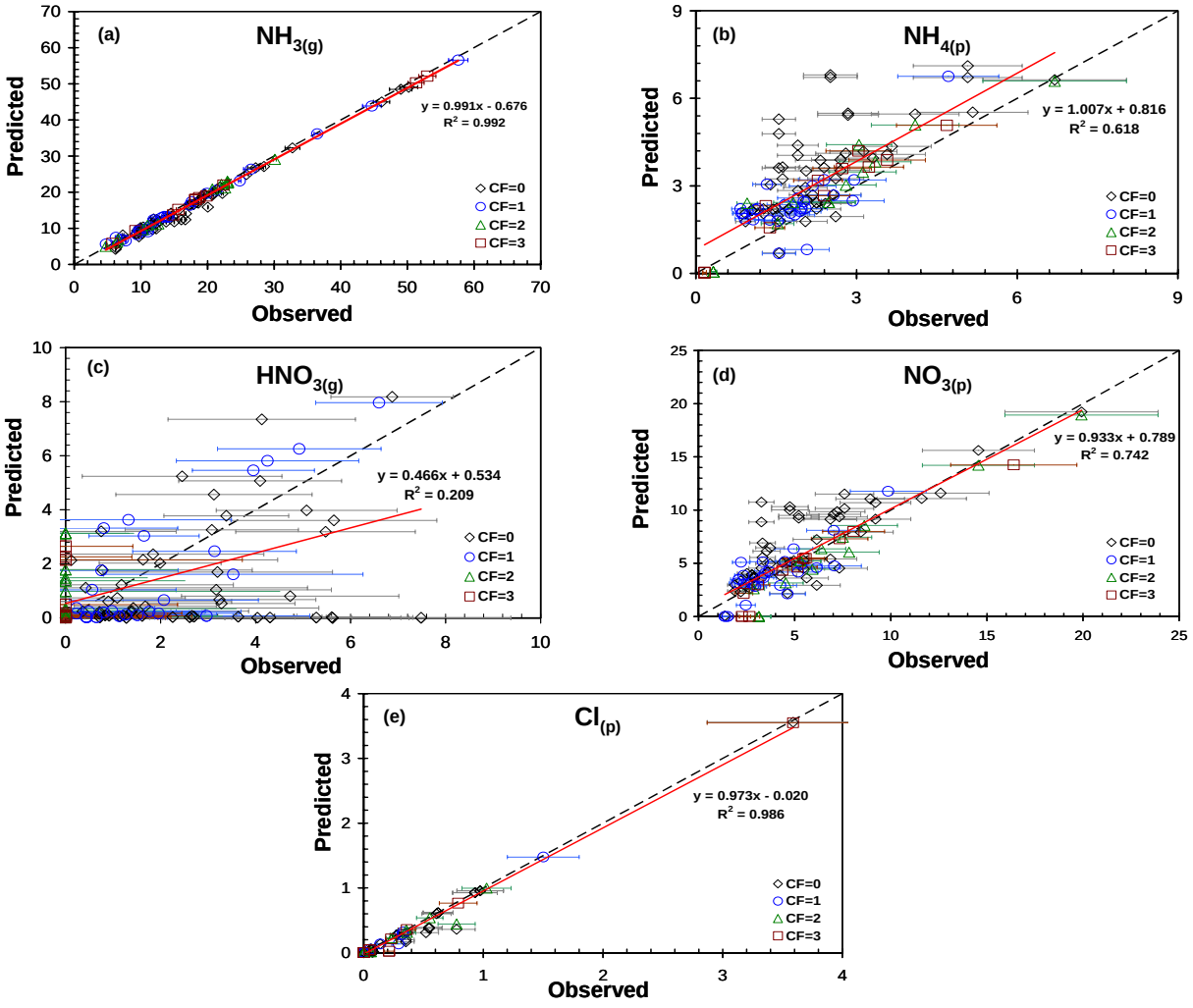

Figure 3. Predicted versus observed concentrations (μg m^{-3}) of (a) $NH_{3(g)}$, (b) $NH_{4(p)}$, (c) $HNO_{3(g)}$, (d) $NO_{3(p)}$, and (e) $Cl_{(p)}$ during the MILAGRO 2006 campaign. Description of legend is given in text. Linear regression line (for all data) is shown for reference. ISORROPIA-II was run assuming stable state solution.

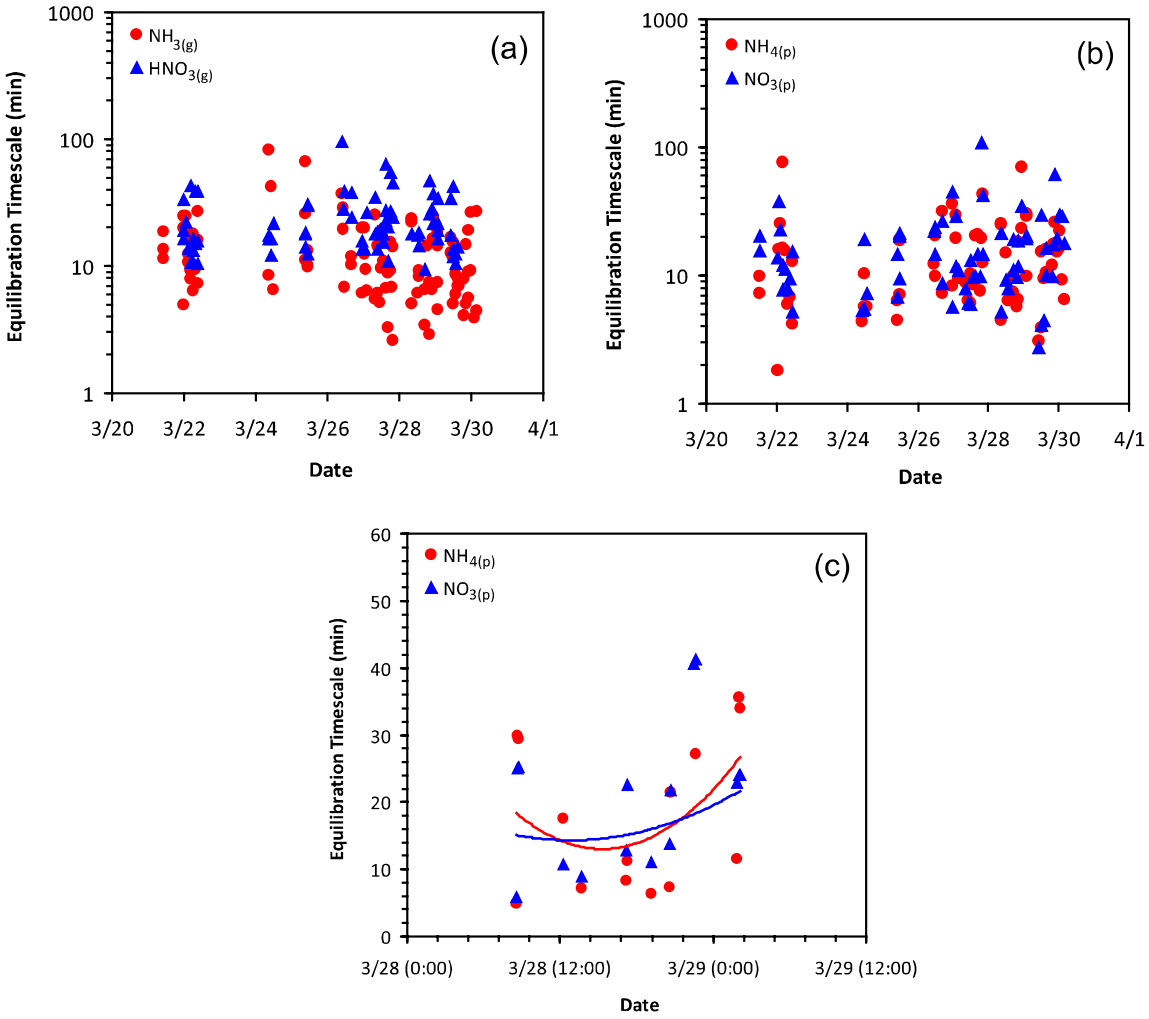

Figure 4. Equilibration timescales for (a) gas-phase, and (b) semivolatile aerosol species during March 2006. Calculations are done assuming a particle size of 1 μm. Also shown (c) are timescales for March 28-29 with polynomial temporal trends.

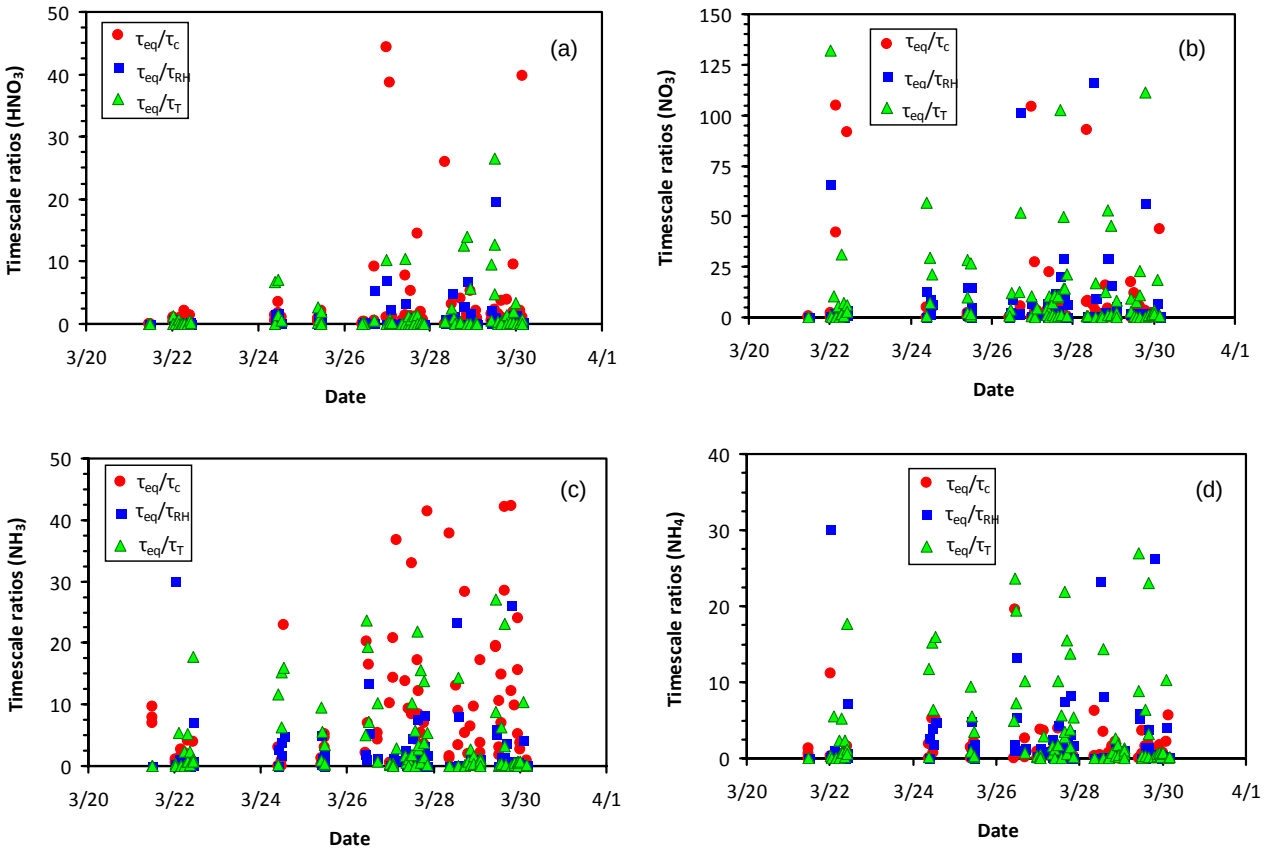

Figure 5. Timescale ratios for (a) gas-phase HNO_3, (b) aerosol NO_3, (c) gas-phase NH_3, and, (d) aerosol NH_4 during the period of March 21-30 2006.

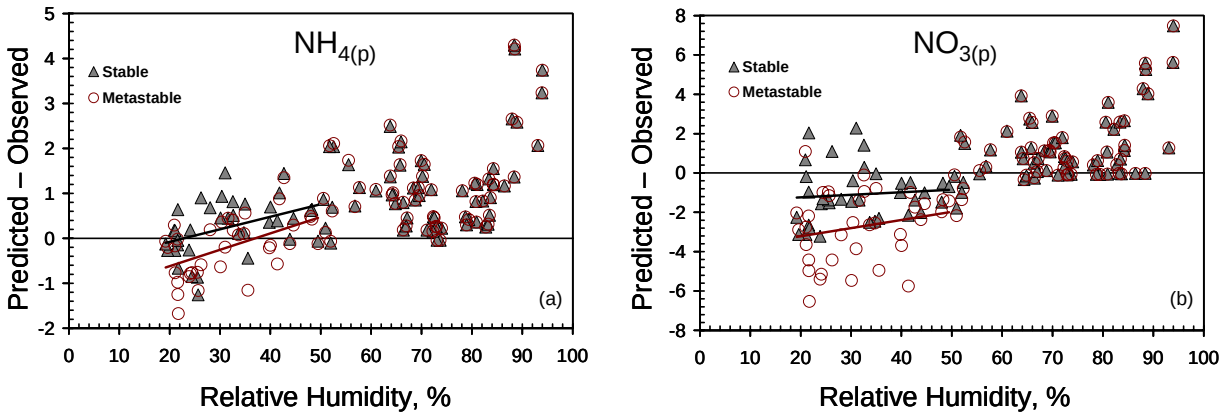

Figure 6. Difference (μg m^{-3}) between predicted and observed concentrations of aerosol (a) ammonium, and, (b) nitrate, as a function of RH using the stable (deliquescence) and metastable solutions of ISORROPIA-II. Linear regression lines are shown for both solutions.

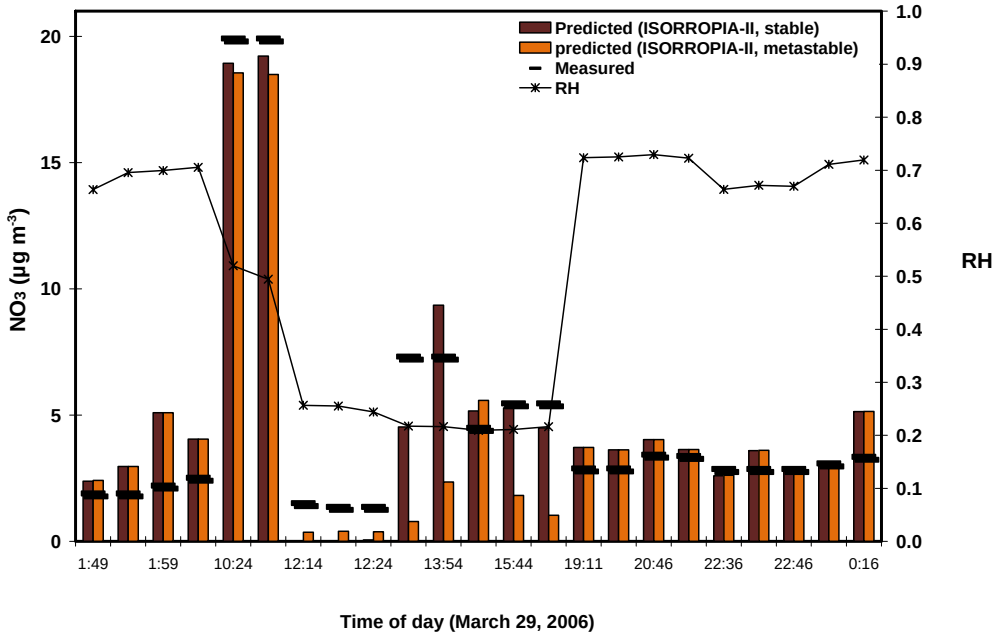

Figure 7. Diurnal profile of aerosol nitrate and RH for March 29, 2006.

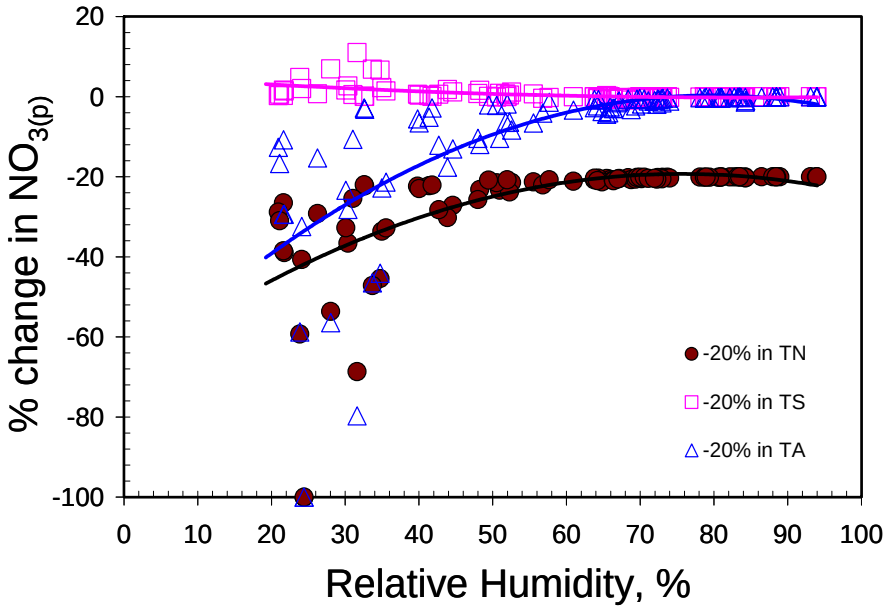

Figure 8. Response of aerosol nitrate predictions of ISORROPIA-II (stable solution; forward mode) to a -20% change in TA, TS and TN as a function of RH. All data (CF=0 - CF=3) are used in the dataset.

1.4 References

Ansari A.S., and S.N. Pandis, Prediction of multicomponent inorganic atmospheric aerosol behavior, Atmos. Environ., 33, 745 - 757, 1999a.

Ansari A.S., and S.N. Pandis, An analysis of four models predicting the partitioning of semivolatile inorganic aerosol components, Aerosol Sci. Technol., 31, 129 - 153, 1999b.

Fitzgerald, J.W., Marine aerosols: A review, Atmos. Environ., 25A, 533 - 545, 1991.

Fountoukis, C. and Nenes, A. (2007) ISORROPIA II: A Computationally Efficient Aerosol Thermodynamic Equilibrium Model for K+, Ca2+, Mg2+, NH4+, Na+, SO42-, NO3-, Cl-, H2O Aerosols, Atmos.Chem.Phys., 7, 4639–4659

Heitzenberg, J., Fine particles in the global troposphere: a review, Tellus 41B, 149 - 160, 1989.

Kim, Y.P., J.H. Seinfeld, and P. Saxena, Atmospheric gas - aerosol equilibrium I. Thermodynamic model, Aerosol Sci. Technol., 19, 157 - 181, 1993a.

Kim, Y.P., J.H. Seinfeld, and P. Saxena, Atmospheric gas - aerosol equilibrium II. Analysis of common approximations and activity coefficient calculation methods, Aerosol Sci. Technol., 19, 182 - 198, 1993b.

Kim, Y.P., and J.H. Seinfeld, Atmospheric gas - aerosol equilibrium III. Thermodynamics of crustal elements Ca^{2+}, K^{+}, and Mg^{2+}, Aerosol Sci. Technol., 22, 93 - 110, 1995.

Moya, M., Fountoukis, C., Nenes, A., Matías, E., and Grutter, M.: Predicting diurnal variability of fine inorganic aerosols and their gas-phase precursors near downtown Mexico City, Atmos. Chem. Phys. Dis., 11257-11294, 2007.

Nenes, A., S.N. Pandis, and C. Pilinis, ISORROPIA: A new thermodynamic equilibrium model for multiphase multicomponent inorganic aerosols, Aquatic Geochemistry, 4, 123 - 152, 1998.

Seinfeld, J.H., and Pandis, S.N.: Atmospheric Chemistry and Physics: From Air Pollution to Climate Change, John Wiley & Sons, Inc., 1998.

2. PUBLICATIONS SUPPORTED BY THIS PROJECT

- Fountoukis, C. and Nenes, A. (2007) ISORROPIA II: A Computationally Efficient Aerosol Thermodynamic Equilibrium Model for K+, Ca2+, Mg2+, NH4+, Na+, SO42-, NO3-, Cl-, H2O Aerosols, Atmos.Chem.Phys., 7, 4639–4659
- Fountoukis, C., Nenes, A., Sullivan, A., Weber, R., VanReken, T., Fischer, M., Matias, E., Moya, M. Farmer, D., and Cohen, R. Thermodynamic characterization of Mexico City Aerosol during MILAGRO 2006, Atmos. Chem. Phys. Discuss.
- Fountoukis, C., Hu, Y., Russell, A., and Nenes, A., On the importance of explicit crustal thermodynamics for PM predictions: A study using CMAQ and ISORROPIA-II, *Atmos.Environ.*, in review

3. CONFERENCE PRESENTATIONS FROM THIS PROJECT

- Fountoukis, C., and A., Nenes, ISORROPIA II: A Computationally Efficient Aerosol Thermodynamic Equilibrium Model for the $K^+ – Ca^{2+} – Mg^{2+} – NH_4^+ – Na^+ – SO_4^{2-} – NO_3^- – Cl^- – H_2O$ System, 7th International Aerosol Conference (IAC), St Paul, Minnesota, September 10-15, 2006.

- Fountoukis, C., and A., Nenes, ISORROPIA II: A Computationally Efficient Aerosol Thermodynamic Equilibrium Model for the $K^+ – Ca^{2+} – Mg^{2+} – NH_4^+ – Na^+ – SO_4^{2-} – NO_3^- – Cl^- – H_2O$ System, Environmental Science/Health Symposium organized by the US Environmental Protection Agency, the Dept. of Energy and the Center for Disease Control, Atlanta, Georgia, April 6, 2006.

- Fountoukis, C., and Nenes, A., "ISORROPIA"-II: A Computationally Efficient Aerosol Thermodynamic Equilibrium Model for the $K^+ – Ca^{2+} – Mg^{2+} – NH_4^+ – Na^+ – SO_4^{2-} – NO_3^- – Cl^- – H_2O$ System", Annual Meeting of the American Institute of Chemical Engineers, San Francisco, CA, November, 2006.

- Karydis, V.A., Tsimpidi, A.P., Nenes, A., Zavala, M., Lei, W., Molina, L.T., Pandis, S.N., "Simulating Inorganic Aerosol Formation using ISORROPIA II in a Chemical Transport Model (PMCAMx) - Evaluation in the Mexico City Metropolitan Area", American Geophysical Union, Fall Meeting, San Fransisco, CA, 2007

- Nenes, A. and Fountoukis, C., "Overview of the ISORROPIA Thermodynamic Model", International Aerosol Modeling Algorithms Conference, Davis, CA, 2007

- Moya, M., C. Fountoukis, A. Nenes, E. Matias, "Is the thermodynamic equilibrium an adequate approach for representing fine (PM1, PM2.5) inorganic aerosol behavior?: ISORROPIA-II simulations under 2005 winter Mexico City conditions", European Aerosol Conference, Salzburg, Austria, 2007